

Application of Spatial-Domain Convolution/Deconvolution Transform for Determining Distance from Image Defocus

Murali Subbarao Nalini B. Agarwal Gopal Surya

Department of Electrical Engineering

State University of New York

Stony Brook, NY 11794-2350

Abstract

This paper describes the application of a new Spatial-Domain Convolution/Deconvolution transform (S transform) for determining distance of objects and rapid autofocusing of camera systems using image defocus. The method of determining distance, named STM, involves simple *local operations* on only a few (about 2 to 4) images and it can be easily implemented in parallel. STM has been implemented on an actual camera system named SPARCS. Experiments on the performance of STM and their results on real-world objects are presented. The results indicate that STM is useful in practical applications. The utility of the method is demonstrated for rapid autofocusing of electronic cameras. STM is computationally more efficient than other methods, but for our camera system, it is somewhat less robust in the presence of noise than a Fourier transform based approach. Although less robust, STM is still a useful technique in many applications such as rapid autofocusing.

Application of Spatial-Domain Convolution/Deconvolution Transform for Determining Distance from Image Defocus

This paper describes the application of a new Spatial-Domain Convolution/Deconvolution transform (S transform) for determining distance of objects and rapid autofocusing of camera systems using image defocus. The method of determining distance, named STM, involves simple *local operations* on only a few (about 2 to 4) images and it can be easily implemented in parallel. STM has been implemented on an actual camera system named SPARCS. Experiments on the performance of STM and their results on real-world objects are presented. The results indicate that STM is useful in practical applications. The utility of the method is demonstrated for rapid autofocusing of electronic cameras. STM is computationally more efficient than other methods, but for our camera system, it is somewhat less robust in the presence of noise than a Fourier transform based approach. Although less robust, STM is still a useful technique in many applications such as rapid autofocusing.

1 Introduction

A new transform named Spatial-Domain Convolution/Deconvolution Transform or S Transform was introduced recently [20]. S transform provides a direct spatial domain method for both convolution and deconvolution of images. It is useful in the restoration of defocused images, and in determining distance of objects from a camera system [21]. In this paper, we describe the application of the S transform for determining distance of objects from a camera using image defocus information.

Determining distance of objects using image defocus information has been investigated by many researchers. Most previous works deal with methods involving processing a large number of images [5, 7, 11, 8], or simple objects such as edges [22, 4, 15, 18], or camera systems with restricted class of point spread functions [9, 16, 17], or computing Fourier coefficients of images Sub89.06. In this paper, a new method named S Transform Method or STM which uses only a few images (about 2 to 4) is presented. It is applicable to arbitrary objects and does not impose restrictions on the point spread function of camera systems. Further, the method does not involve the computation of Fourier coefficients of images.

In addition to being novel, STM has one important advantage over existing methods in that it involves only local operations on images. Therefore it can yield denser depth-maps, and it can be easily implemented in parallel.

STM has been implemented on an actual camera system named Stonybrook Passive Autofocusing and Ranging Camera System or SPARCS. Experiments on SPARCS and their results are described. The results indicate that STM is useful in practical applications such as passive ranging in robotic vision and rapid autofocusing of camera systems.

Next section describes the camera model and image defocus model used in this paper. The following section defines S transform and summarizes some results relevant to STM. Section 4 deals with the detailed theory of STM. Implementation of STM, experiments, and their results are presented in the subsequent sections.

2 Camera model

Image formation in a simple camera is shown in in Fig. 1. Let P be a point on a visible surface in the scene and p be its focussed image. The relation between the positions of P and p is given by the lens formula,

$$\frac{1}{f} = \frac{1}{u} + \frac{1}{v} \quad (1)$$

where u is the object distance and v is the image distance. If P is not in focus it gives rise to a blurred image. According to geometric optics, the blurred image of P has the same shape as the lens aperture but scaled by a factor. Let the blurred image of the point P be $h(x, y)$. Clearly $h(x, y)$ is the response of the camera to a point source and hence $h(x, y)$ is the point spread function.

Usually camera systems have a circular aperture. In this case the blurred image of a point on the image detector is circular in shape and is called the *blur circle*. Let R be the radius of the blur circle and D be the diameter of the lens aperture, and s be the distance from the lens to the image detector plane (Fig. 1). Also let q be the scaling factor defined $q = 2R/D$. In Fig. 1, from similar triangles we have

$$q = \frac{2R}{D} = \frac{s - v}{v} = s \left[\frac{1}{v} - \frac{1}{s} \right] \quad (2)$$

Substituting for $1/v$ from Eq. (1) in the above equation, we obtain

$$q = s \left[\frac{1}{f} - \frac{1}{u} - \frac{1}{s} \right] \quad (3)$$

Therefore

$$R = q \frac{D}{2} = s \frac{D}{2} \left[\frac{1}{f} - \frac{1}{u} - \frac{1}{s} \right] \quad (4)$$

Note that q and therefore R can be either positive or negative depending on whether $s \geq v$ or $s < v$. In the former case the image detector plane is behind the focused image of P and in the latter case it is in front of the focused image of P .

According to geometric optics, the intensity within the blur circle is approximately constant. If we further assume the camera to be lossless system (i.e., no light energy is absorbed by the camera system) we get

$$h_1(x, y) = \begin{cases} \frac{1}{\pi R^2} & \text{if } x^2 + y^2 \leq R^2 \\ 0 & \text{otherwise} \end{cases} \quad (5)$$

where $h_1(x, y)$ is the point spread function of the camera, derived using geometric optics.

Taking diffraction and non-idealities of lenses into account, an alternative model has been suggested for the intensity distribution given by a two dimensional Gaussian [12, 9, 17],

$$h_2(x, y) = \frac{1}{2\pi\sigma^2} e^{-\frac{1}{2}\frac{x^2+y^2}{\sigma^2}} \quad (6)$$

where σ is the spread parameter such that

$$\sigma = k R \text{ for } k > 0. \quad (7)$$

k is a constant of proportionality characteristic of the given camera. In except when σ is very small (in which case diffraction effects dominate), in most practical cases

$$k = \frac{1}{\sqrt{2}} \quad (8)$$

is a good approximation [19, 15, 18].

If the radius R is a constant over some region on the image plane, the camera acts as a linear shift invariant system. This is justified because the camera parameters s, D and f all remain the same. Therefore the observed image $g(x, y)$ is the result of convolving the corresponding focused image $f(x, y)$ with the camera's point spread function $h(x, y)$, i.e.,

$$g(x, y) = h(x, y) * f(x, y) \quad (9)$$

where $*$ denotes the convolution operation.

The point spread functions h_1 and h_2 defined above are only two specific examples used to clarify our method. In order to deal with other forms of point spread functions, we use the spread parameter σ_h to characterize them where σ_h is the standard deviation of the distribution of any function h .

Using the polar co-ordinate system it can be shown [15] that the spread parameter σ_{h_1} corresponding to h_1 is $R/\sqrt{2}$. Therefore from equation (4) we have

$$\sigma_{h_1} = mu^{-1} + c \quad (10)$$

where

$$m = -\frac{Ds}{2\sqrt{2}} \quad (11)$$

and

$$c = \frac{Ds}{2\sqrt{2}} \left[\frac{1}{f} - \frac{1}{s} \right] \quad (12)$$

We see that for a given camera setting (i.e., for a given value of the camera parameters s, f, D) the spread parameter σ_h depends linearly on inverse distance u^{-1} . Similarly it can be shown that the spread parameter σ_{h_2} of h_2 is σ . Therefore from equations (7), (8) and (4) we again obtain

$$\sigma_{h_2} = mu^{-1} + c. \quad (13)$$

In fact it has been shown in [18] that even for an arbitrarily shaped aperture, σ_h is linearly related to inverse distance u^{-1} .

3 S Transform

A detailed discussion of S transform can be found in [20]. In this section we summarize some results relevant to STM. First we introduce some notation, and then present the results.

P_2^{N+1} : Space of all real valued two-dimensional polynomial functions of degree less than or equal to N for $N = 0, 1, 2, 3, \dots$.

For x, y real and any function real $f(x, y)$,

$$f^{m,n} \equiv \frac{\partial^m}{\partial x^m} \frac{\partial^n}{\partial y^n} f(x, y). \quad (14)$$

Two-dimensional N -th order polynomial:

$$f(x, y) = \sum_{m=0}^N \sum_{n=0}^{N-m} a_{m,n} x^m y^n \quad (15)$$

$$= \sum_{0 \leq m+n \leq N} a_{m,n} x^m y^n. \quad (16)$$

If $f \in P_2^{N+1}$, then

$$f^{m,n} = 0 \quad \text{for} \quad m + n > N. \quad (17)$$

Two-dimensional moments:

$$h_{m,n} \equiv \int_{-\infty}^{\infty} \int_{-\infty}^{\infty} x^m y^n h(x,y) dx dy \quad (18)$$

for $m, n = 0, 1, 2, 3, \dots$.

M_2^{N+1} : the space of all real valued functions $h(x,y)$ such that $h_{0,0} \neq 0$ and all moments of h upto order N are finite, i.e.,

$$|h_{m,n}| < \infty \quad \text{for } m+n = 0, 1, 2, \dots, N. \quad (19)$$

Forward S transform of $f(x,y)$ with respect to $h(x,y)$:

$$F_H(x,y) = h(x,y) * f(x,y) \quad (20)$$

$$= \sum_{0 \leq m+n \leq N} \frac{(-1)^{m+n}}{m!n!} f^{m,n} h_{m,n} \quad (21)$$

where $h_{m,n}$ is as defined in Eq. (18).

Inverse S transform of $F_H(x,y)$ with respect to $h(x,y)$:

$$f(x,y) = \sum_{k=0}^N \sum_{l=0}^k w_{k-l,l} F_H^{k-l,l} = \sum_{k=0}^N \sum_{0 \leq i+j \leq k} w_{i,j} F_H^{i,j} \quad (22)$$

$$w_{i,j} = \sum \frac{(-1)^{p+i+j}}{h_{0,0}^{p+1}} \prod_{q=1}^p \left(\frac{h_{m_q, n_q}}{m_q! n_q!} \right) \quad (23)$$

where, in the above equation, summation is done over all possible m_q, n_q, p , for $q = 1, 2, 3, \dots, p$, subject to the conditions

$$\left[\begin{array}{l} m_1 + m_2 + \dots + m_p = i \\ n_1 + n_2 + \dots + n_p = j \\ m_1 + n_1 \geq 1, m_2 + n_2 \geq 1, \dots, m_p + n_p \geq 1 \end{array} \right]. \quad (24)$$

(We apologize, for we could not find a simpler notation/representation for the inverse S transform. Derivation of this transform and examples can be found in [20, 21]. For the purposes of this paper, $N \leq 3$. If you have patience, it is not difficult (but tedious) to verify the inverse transform.)

4 Determining Distance by STM

STM is based on approximating the image function $f(x, y)$ as a polynomial function in small regions. (Note: At least in principle, for any given analytic function, a polynomial arbitrarily close to it exists, according to a famous theorem by Weierstrass, as is well known in Approximation Theory.) In our application, usually a third order polynomial approximation in image neighborhoods of size about 9×9 pixels suffices. This assumption is specified by

$$f(x, y) = \sum_{0 \leq m+n \leq 3} a_{m,n} x^m y^n \begin{cases} A1 \leq x \leq A2 \\ B1 \leq y \leq B2 \end{cases} \quad (25)$$

From equations (9) and (21) we have the blurred image,

$$g(x, y) = h(x, y) * f(x, y) = \sum_{0 \leq m+n \leq 3} \frac{(-1)^{m+n}}{m! n!} h_{m,n} f^{m,n}. \quad (26)$$

Assuming $h(x, y)$ is circularly symmetric, it can be shown that

$$h_{m,n} = 0 \quad \text{for } (m \text{ odd}) \text{ or } (n \text{ odd}) \text{ and } h_{m,n} = h_{n,m}. \quad (27)$$

For any point spread function,

$$h_{0,0} = 1 \quad (28)$$

From equations (26) and (28), $g(x, y)$ becomes

$$g(x, y) = f^{0,0} + \frac{1}{2!} h_{2,0} f^{2,0} + \frac{1}{2!} h_{0,2} f^{0,2} \quad (29)$$

In order to use the inverse S transform for this case we can write down the weights $w_{i,j}$ from equation (23) as

$$w_{0,0} = \frac{1}{h_{0,0}} \quad (30)$$

$$w_{0,1} = \frac{h_{0,1}}{h_{0,0}^2} \quad (31)$$

$$w_{1,0} = \frac{h_{1,0}}{h_{0,0}^2} \quad (32)$$

$$w_{0,2} = \frac{h_{0,1}^2}{h_{0,0}^3} - \frac{h_{0,2}}{2h_{0,0}^2} \quad (33)$$

$$w_{1,1} = \frac{h_{0,1}h_{1,0}}{h_{0,0}^3} - \frac{h_{1,1}}{h_{0,0}^2} \quad (34)$$

$$w_{2,0} = \frac{h_{1,0}^2}{h_{0,0}^3} - \frac{h_{2,0}}{2h_{0,0}^2}. \quad (35)$$

From equation (27) we have $h_{0,1} = h_{1,0} = h_{1,1} = 0$ and $h_{2,0} = h_{0,2}$. Substituting these values of $h_{m,n}$ in the expressions for $w_{i,j}$ above, and using Eq. (22) we get

$$f(x, y) = g(x, y) - \frac{h_{0,2}}{2} \{g^{2,0}(x, y) + g^{0,2}(x, y)\} \quad (36)$$

From the definition of moments and σ_h we have $h_{0,2} = h_{2,0} = \sigma_h^2/2$. So

$$f(x, y) = g(x, y) - \frac{\sigma_h^2}{4} \{g^{2,0}(x, y) + g^{0,2}(x, y)\} \quad (37)$$

Let us consider a blurred image $g_1(x, y)$ of the object and let σ_1 be the corresponding spread parameter. From equation (10) we can write

$$\sigma_1 = m_1 u^{-1} + c_1 \quad (38)$$

where

$$m_1 = -\frac{D_1 s_1}{2\sqrt{2}} \text{ and } c_1 = \frac{D_1 s_1}{2\sqrt{2}} \left[\frac{1}{f_1} - \frac{1}{s_1} \right]. \quad (39)$$

Similarly for a second blurred image $g_2(x, y)$ we can write

$$\sigma_2 = m_2 u^{-1} + c_2 \quad (40)$$

where

$$m_2 = -\frac{D_2 s_2}{2\sqrt{2}} \text{ and } c_2 = \frac{D_2 s_2}{2\sqrt{2}} \left[\frac{2}{f_2} - \frac{2}{s_2} \right]. \quad (41)$$

Therefore,

$$u^{-1} = \frac{\sigma_1 - c_1}{m_1} = \frac{\sigma_2 - c_2}{m_2}. \quad (42)$$

σ_1 can then be expressed in terms of σ_2 as

$$\sigma_1 = \alpha \sigma_2 + \beta. \quad (43)$$

where

$$\alpha = \frac{m_1}{m_2} \text{ and } \beta = c_1 - c_2 \frac{m_1}{m_2}. \quad (44)$$

Now, the original (focused) image $f(x, y)$ can be expressed in terms of $g_1(x, y)$ using equation (37) as

$$f = g_1^{0,0} - \frac{1}{4} \sigma_1^2 (g_1^{0,2} + g_1^{2,0}) \quad (45)$$

Similarly $f(x, y)$ can also be expressed in terms of a second blurred image $g_2(x, y)$ as

$$f = g_2^{0,0} - \frac{1}{4} \sigma_2^2 (g_2^{0,2} + g_2^{2,0}) \quad (46)$$

Equating the right hand sides of equations (45) and (46) we have

$$g_1^{0,0} - \frac{1}{4} \sigma_1^2 (g_1^{0,2} + g_1^{2,0}) = g_2^{0,0} - \frac{1}{4} \sigma_2^2 (g_2^{0,2} + g_2^{2,0}) . \quad (47)$$

Using relations (43) and (47) we obtain,

$$a \sigma_2^2 + b \sigma_2 + c = 0 \quad (48)$$

where

$$a = \frac{1}{4} \left\{ \alpha^2 (g_2^{0,2} + g_2^{2,0}) - (g_1^{0,2} + g_1^{2,0}) \right\} \quad (49)$$

$$b = \frac{1}{2} \alpha \beta (g_2^{0,2} + g_2^{2,0}) \quad (50)$$

$$c = (g_1^{0,0} - g_2^{0,0}) + \frac{1}{4} \beta^2 (g_2^{0,2} + g_2^{2,0}) \quad (51)$$

Note that $(g^{0,2} + g^{2,0}) = \nabla^2 g$ corresponds to the Laplacian operation on the image $g(x, y)$. The values of α and β are determined using the camera parameter values in relations (39), (41) and (44). The Laplacians $\nabla^2 g_1$ and $\nabla^2 g_2$ are computed from the two observed images g_1 and g_2 . Therefore, the coefficients a , b and c can be computed from a knowledge of the camera parameters and the observed images using relations (49), (50) and (51). Having computed the coefficients a , b and c , we can solve for σ_2 by solving the quadratic equation (48). The distance u of the object is then obtained from equation (40).

Every pixel of the 64×64 image gives rise to two values of object distance u . Ideally every pixel should give rise to the same set of values of u . This happens if the polynomial approximation of the image, in a small neighbourhood around the pixel, is good enough. But in practice there will be some pixels giving rise to different

values of u . In order to deal with this problem, a histogram of the number of pixels versus object distance is generated. The mode of the histogram, is then taken to be the actual value of u . In a sense, each pixel votes for a value of u . The value of u which receives the maximum number of votes, is chosen to be the actual value.

5 STM Implementation

STM described above was implemented on a camera system named Stonybrook Passive Autofocusing and Ranging Camera System (SPARCS). SPARCS was built over the last two years in the Computer Vision Laboratory at the Department of Electrical Engineering, State University of New York, Stony Brook. A block diagram of the system is shown in Figure 2. SPARCS consists of a SONY XC-711 CCD camera and an Olympus 35-70mm motorized lens. Images from the camera are captured by a frame grabber board (Quickcapture DT2953 of Data Translation). The frame grabber board resides in an IBM PS/2 (model 70) personal computer. The images taken by the frame grabber are processed in the PS/2 computer.

The focal length of the lens can be varied manually from about 35mm to 70mm. The F-number which is defined as the ratio of the focal length f to aperture diameter D can also be set manually to 4, 8, 22 etc.,. The lens system consists of multiple lenses and focusing is done by moving the front lens forward and backward. The lens can be moved either manually or under computer control. To facilitate computer control of the lens movement there is a stepper motor with 97 steps, numbered 0 to 96. Step number 0 corresponds to focusing an object at distance infinity and step number 96 corresponds to focusing a nearby object, at a distance of about 50cm from the lens. The motor is controlled by a microprocessor, which can communicate with the IBM PS/2 through a digital I/O board (Contec mPIO24/24). Pictures taken by the camera can be displayed in real time on a color monitor (SONY PVM-1342 Q). The images acquired and stored in the IBM PS/2 can be transferred to a SUN workstation.

As mentioned earlier, there are 97 step positions for the stepper motor, and there-

fore there are 97 distinct focusing positions of the lens. For each position of the lens, there corresponds a unique distance which is such that an object placed at that distance from the camera would be in focus. For convenience shall use lens step positions to specify and measure distances. For example, if the distance of an object is said to be step 30, by this we mean that the distance of the object is such that if the lens is moved to step number 30, then the object would be in best focus.

The first step in the implementation of STM is to find the camera constants m_1, c_1 and m_2, c_2 . There are two different ways of determining these constants. One method which was already mentioned is to use relations (39) and (41). This requires accurate knowledge of the camera parameters. The second method is to determine them experimentally [15]. The experimental method is briefly outlined next.

5.1 Camera Calibration

In our experiments, only one camera parameter, the lens position s was varied. All other parameters (focal length f and aperture diameter D) were almost nearly constant. In the experiments, three different lens positions corresponding to step numbers 10, 40, and 70 were chosen. For each position of the lens, the object distance was varied from step number 0 to 95 at 5 step intervals. The object was chosen to be a step edge created by pasting black and white papers on a cardboard. For each distance of the object, the parameter σ was measured. More details on this part can be found in [15, 18]. The data thus obtained for lens step positions 10, 40, and 70 are shown in Figures 3, 4, and 5, respectively. The slope and the intercepts of the linear parts of these plots give the values of m and c respectively.

5.2 Experiments

A typical object was placed in front of the SPARCS camera. Three images of the object were obtained for three lens positions of steps 10, 40, and 70. A subimage of size 64×64 from the center of each of the the three images were extracted for further processing. The three images were normalized with respect to brightness by

normalizing their mean grey levels to unity.

In order to reduce the effects of noise, the images were smoothed using the smoothed unweighted differentiation filters suggested in [23]. The filter size was 9×9 . The same filters were used for estimating the Laplacian of the images.

Next the coefficients a , b , and c were calculated for images taken at steps 10 and 40. The solution for σ_2 was then obtained. The distance of the object was obtained from the solution for σ_2 . In our experiments, due to the cubic polynomial model for the image $f(x, y)$, the Laplacians of g_1 and g_2 were the same, and also $\alpha = 1.0$. Therefore, the coefficient a was always zero. For this reason, the solution for σ_2 and hence the solution for distance were always unique. Next the same calculations were repeated for images taken at lens positions 40 and 70 to check for consistency of the results.

One value of distance was calculated from each image neighborhood where the Laplacian was more than a specified threshold. A histogram of the values thus computed at different pixels were computed. The mode of the histogram was taken to be the most likely estimate of distance of the object.

The experiment described above was performed on three different objects: poster of a tiger (Fig. 6), a binary image with printed text (Fig. 7), and a teddy bear (Fig. 8). The results are plotted in Figs. 9, 10, and 11 respectively. The actual distance of the object measured in step numbers is along the x axis, and the estimated distance is along the y axis. Under ideal conditions, the plots would have been diagonals running from bottom-left to top-right. The experimental results, especially for the tiger's face poster, are generally good. The bad points in the graph are probably due to our assumption that the image can be locally modeled as a cubic polynomial. Large errors will result in places where this assumption is in gross error.

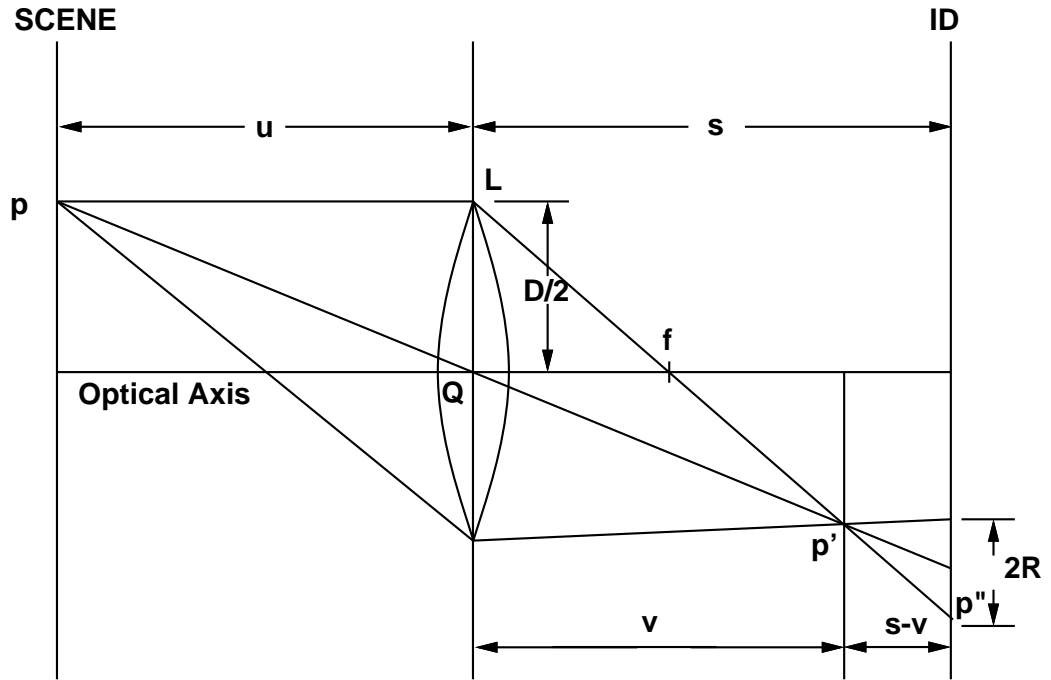
The camera settings used in the experiment were

- Focal Length = 35mm.
- F- Number = 4.
- Camera Gain Control = +6dB.

- White Balance = Off.
- Gamma Compensation = Off.

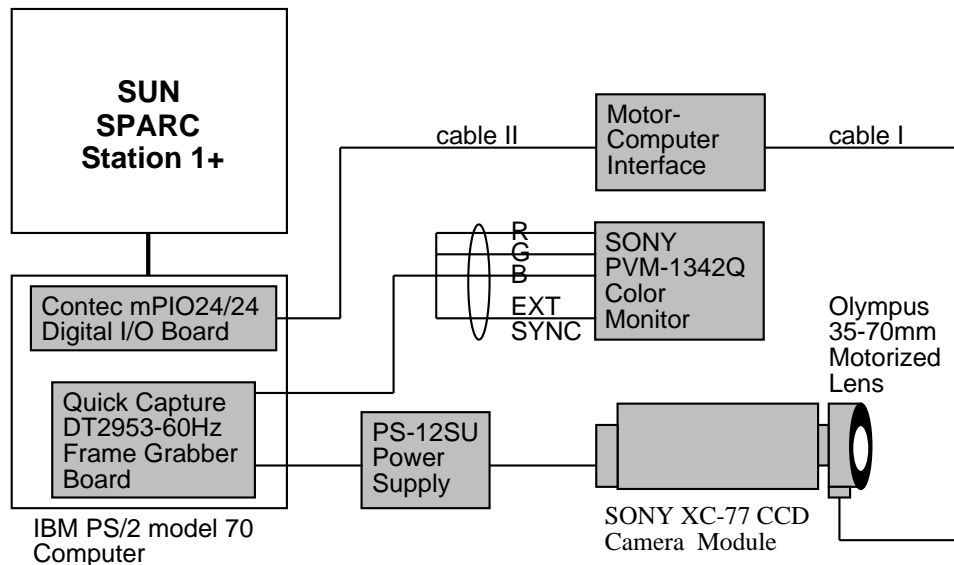
6 Conclusions

STM is more accurate for nearby objects than for farther objects. This is a common characteristic of all Depth-from-Defocus methods. Integration of STM with Depth-from-Stereo can reduce the computations involved in Depth-from-Stereo which is about an order of magnitude more accurate than STM. STM illustrates one application of S transform. Another application in image restoration is currently under investigation.



L Lens **Q** Optical Center **D** Aperture Diameter
p Object **p'** Focused Point **f** Focal Length
ID Image Detector **p''** Blur Circle **R** Blur Circle Radius

Fig.1 Image Formation in a Simple Camera System

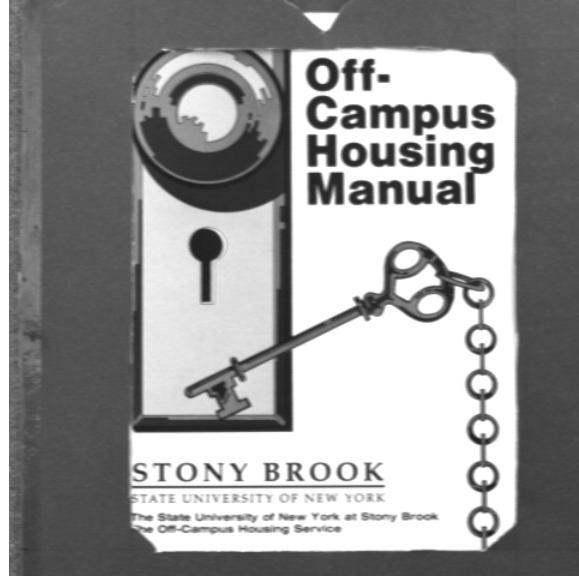


Stonybrook Passive Autofocusing and Ranging Camera System- SPARCS - is a prototype camera system developed at the Computer Vision Laboratory for experimental research in robotic vision, State University of New York at Stony Brook.

Fig.2 Block Diagram of SPARCS



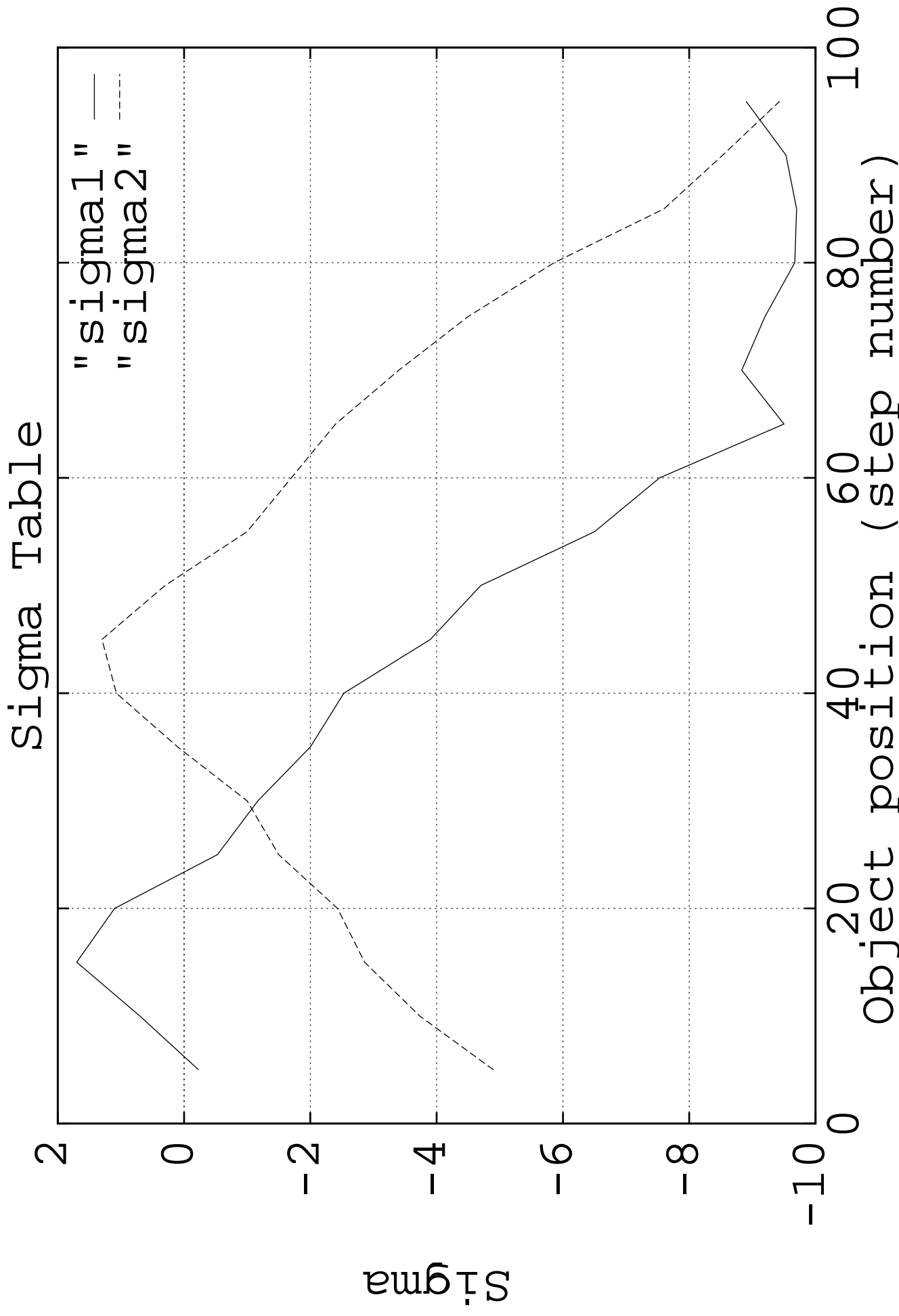
OBJECT 1: TIGER'S FACE



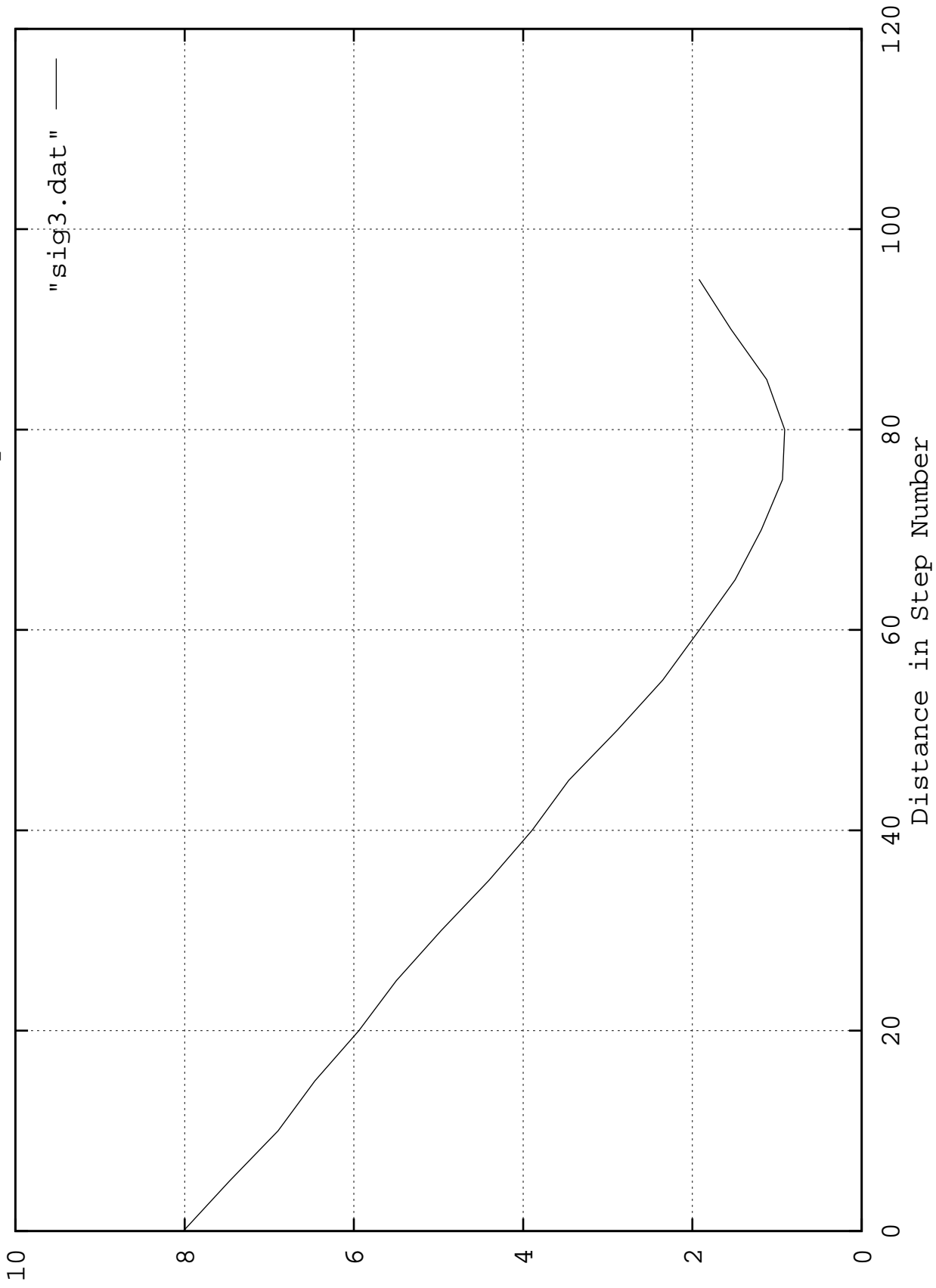
OBJECT 2: BINARY IMAGE



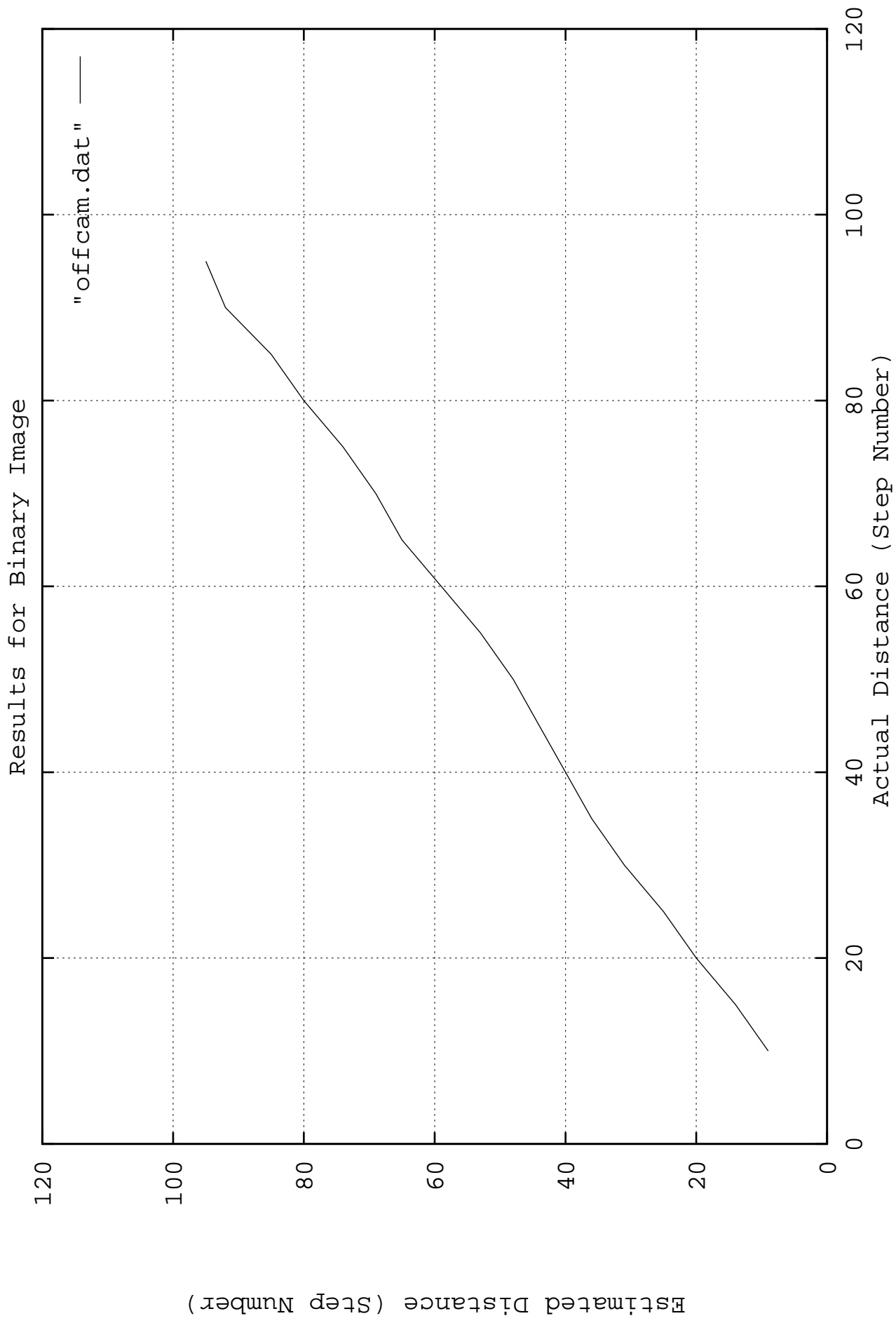
OBJECT 3: A 3-D OBJECT(DOLL)



Calibration Data for Step 70



SIGMA



References

- [1] B. Topielski, *A Computer Controlled Lens Positioning System for Autofocusing*, Unpublished report prepared as part of a senior design project, Computer Vision Laboratory, Dept. of Electrical Engg., SUNY, Stony Brook, NY 11794-2350.
- [2] J. D. Gaskill, *Linear Systems, Fourier Transforms, and Optics*, John Wiley & Sons, New York, 1978.
- [3] J. W. Goodman, *Introduction to Fourier Optics*, McGraw-Hill, Inc., 1968.
- [4] P. Grossman, “Depth from focus”, *Pattern Recognition Letters* 5, pp. 63–69, Jan. 1987.
- [5] B. K. P. Horn, “Focusing”, Artificial Intelligence Memo No. 160, MIT, 1968.
- [6] B. K. P. Horn, *Robot Vision*, McGraw-Hill Book Company, 1986.
- [7] R. A. Jarvis, “A perspective on range finding techniques for computer vision”, *IEEE Transactions on Pattern Analysis and Machine Intelligence*, PAMI-5, No. 2, pp. 122–139, March 1983.
- [8] E. Krotkov, “Focusing”, *International Journal of Computer Vision*, 1, 223-237, 1987.
- [9] A. P. Pentland, “A new sense for depth of field”, *IEEE Transactions on Pattern Analysis and Machine Intelligence*, Vol. PAMI-9, No. 4, pp. 523–531.
- [10] A. Rosenfeld, and A. C. Kak, *Digital Picture Processing*, Vol. I . Academic Press, 1982.
- [11] J. F. Schlag, A. C. Sanderson, C. P. Neuman, and F. C. Wimberly, “Implementation of automatic focusing algorithms for a computer vision system with

camera control”, CMU-RI-TR-83-14, Robotics Institute, Carnegie-Mellon University, 1983.

- [12] W. F. Schreiber, *Fundamentals of Electronic Imaging Systems*, Springer-Verlag, Section 2.5.2., 1986.
- [13] M. Subbarao, and A. Nikzad, “A model for image sensing and digitization in machine vision”, OE/BOSTON '90, SPIE conference, Boston, Nov. 1990.
- [14] M. Subbarao, “Computational methods and electronic camera apparatus for determining distance of objects, rapid autofocusing, and obtaining improved focus images”, U.S. patent application serial number 07/373,996, June 1989 (pending).
- [15] M. Subbarao, and G. Natarajan, “Depth recovery from blurred edges”, *Proceedings of the IEEE Computer Society Conference on Computer Vision and Pattern Recognition*, Ann Arbor, Michigan, pp. 498-503, June 1988.
- [16] M. Subbarao, “Parallel depth recovery by changing camera parameters”, *Second International Conference on Computer Vision*, Florida, USA, pp. 149-155, December 1988.
- [17] M. Subbarao, “Efficient depth recovery through inverse optics”, Editor: H. Freeman, *Machine Vision for Inspection and Measurement*, Academic press, Boston, pp. 101-126, 1989.
- [18] M. Subbarao, “Determining distance from defocused images of simple objects”, Tech. Report No. 89.07.20, Computer Vision Laboratory, Dept. of Electrical Engineering, State University of New York, Stony Brook, NY 11794-2350.
- [19] M. Subbarao, “On the depth information in the point spread function of a defocused optical system”, Tech. Report No. xx.xx.xx, Computer Vision Laboratory, Dept. of Electrical Engineering, State University of New York, Stony Brook, NY 11794-2350.

- [20] M. Subbarao, "Spatial-Domain Convolution/Deconvolution Transform ", Tech. Report No. 91.07.03, Computer Vision Laboratory, Dept. of Electrical Engineering, State University of New York, Stony Brook, NY 11794-2350. (Also submitted to *IEEE Transactions on Signal Processing*).
- [21] M. Subbarao, *Passive Ranging and Rapid Autofocusing*, U.S. patent application serial no. 07/551,933, filing date 07/12/90 (pending).
- [22] J. M. Tenenbaum, *Accommodation in Computer Vision*, Ph.D. Dissertation, Stanford University, Nov. 1970.
- [23] P. Meer and I. Weiss, *Smoothed differentiation filters for images*, Tech. Report No. CS-TR-2194, Center for Automation Research, University of Maryland, College Park, MD 20742-3411.